

**LA-UR-24-22087**

**Approved for public release; distribution is unlimited.**

**Title:** Silicone Resins for Vat Polymerization Printing

**Author(s):** Hurlbutt, Katey Marie

**Intended for:** Report

**Issued:** 2024-03-08 (rev.1)



Los Alamos National Laboratory, an affirmative action/equal opportunity employer, is operated by Triad National Security, LLC for the National Nuclear Security Administration of U.S. Department of Energy under contract 89233218CNA00001. By approving this article, the publisher recognizes that the U.S. Government retains nonexclusive, royalty-free license to publish or reproduce the published form of this contribution, or to allow others to do so, for U.S. Government purposes. Los Alamos National Laboratory requests that the publisher identify this article as work performed under the auspices of the U.S. Department of Energy. Los Alamos National Laboratory strongly supports academic freedom and a researcher's right to publish; as an institution, however, the Laboratory does not endorse the viewpoint of a publication or guarantee its technical correctness.

# Silicone Resins for Vat Polymerization Printing

Katey M. Hurlbutt\*

Los Alamos National Laboratory, New Mexico 87545

*KEYWORDS: Silicones, polymerization, additive manufacturing, vat polymerization printing*

---

**ABSTRACT:** This paper reviews research of silicone-based resins for vat polymerization printing (VPP). Silicone resins are used commonly in other 3D printing technologies because of their desirable properties. Silicones are chemically inert, oxidatively, and thermally stable, and have the lowest glass transition temperature of any polymer. Creating silicone resins processable by VPP is challenging because VPP requires low viscosity liquid resin that quickly photopolymerizes. This review will summarize VPP technologies, resin chemistries, and recent research of silicone VPP resins.

---

## Technology Overview

Additive manufacturing (AM) technologies have improved significantly in recent years, creating new markets and possibilities for research. AM involves fusing material layer by layer based on computer aided design (CAD). Developed in the 1980s for “rapid prototyping”, AM created new markets by quickly producing inexpensive, unique and low volume parts<sup>1</sup>. The global AM market was estimated to be worth \$12 billion in 2012, and is projected to grow to \$78 billion by 2028<sup>1</sup>. AM encompasses a diverse set of technologies, including extrusion of melted or high viscosity flowable materials, fusion of powders, and photo-initiated curing of low viscosity resins. The focus of this paper is vat polymerization of silicone resins.

Polymers are molecules made up of linked repeating units called monomers. Resins for AM contain polymer precursors, which may be “oligomers,” a molecule consisting of a few monomers linked together, or “macromers,” which consist of many monomers linked together. Vat polymerization printing (VPP) of polymers uses light to initiate polymerization of a layer of liquid polymer resin. The print bed is then moved up through the vat of resin or down into it, and the next layer is polymerized<sup>2</sup>. The polymer precursors in VPP resins may have UV reactive functional groups, or the formulation may contain a photoinitiator, the latter of which is more common<sup>3</sup>. VPP can provide the highest resolution of parts because the technology is not limited by nozzle sizes or pressures the way extrusion-based printing technologies are. VPP isn’t one technology, but rather a broad category of AM. Subcategories of vat polymerization

include stereolithography (SL), digital light processing (DLP), continuous liquid interface production (CLIP), and multiphoton polymerization (MPP).

Stereolithography uses a laser to scan over the surface of liquid photo-curable polymer resin. Stereolithography was among the first additive manufacturing technologies developed. It was patented in the US in 1984 by Chuck Hill<sup>4</sup>, and the first commercial machines were available shortly after<sup>5</sup>.

Digital light processing exposes the resin to a 2D image representing an entire layer, making it considerably faster than stereolithography<sup>2</sup>. This technology was developed in 1987 by Larry Hornbeck and was brought to market in 1996<sup>6</sup>. Both SL and DLP require a step of detaching the polymerized layer from the build window. This step takes time, and the build object can fail to detach or be damaged in the process. CLIP improves DLP by solving this issue with an oxygen permeable window at the bottom of the resin vat. Many polymerization systems are inhibited by oxygen, so the layer of resin in which the oxygen diffuses does not polymerize. This prevents the build from adhering to the window, eliminating the detachment step<sup>6</sup>. CLIP is a new technology; patented by Joseph DeSimone in 2014<sup>7,8</sup>.

In DLP and SL, the intensity of light experienced by the polymer resin is directly proportional to the depth. Thus, as the light penetrates deeper into the resin, the intensity decreases linearly. This results in ‘blurry’ layers. Multiphoton polymerization reduces this blurriness, improving resolution. In this technique, two laser beams focus on a single point and scan over the print layer together. Resins must absorb two or more photons to initiate polymerization, which occurs only at the focal

point of both beams. With MPP resins, the intensity of light decreases exponentially with increasing distance from the focal point of the beams<sup>2</sup>. This allows finer control of the polymerization<sup>9</sup>. The theoretical basis of multiphoton printing dates back to a 1931 paper by Maria Göppert-Mayer, in which she described the possibility and challenges associated with multiphoton excitation<sup>10</sup>. Technology enabling these techniques began to develop in the 60s. In 1965, a paper was published describing the polymerization of styrene using a laser<sup>8</sup>, and in 1991 the first experiments were conducted using this technology to produce three-dimensional objects<sup>11</sup>.

### Material Overview

The resolution, material and chemical properties of the build are determined as much by the chemistry of the polymer resin as by the AM technology used. The first resins used for VPP were not created for this new technology. The 1984 Hull patent describes using UV curable adhesive as the resin<sup>1</sup>. Early resins consisted of low molecular weight precursors, producing polymers with high crosslink density. Objects produced with these resins are hard and brittle. Today, the formulations of commercial resins are trade secrets, but patents reveal common primary components of VPP resins are acrylates, methacrylates, and epoxies<sup>12</sup>.

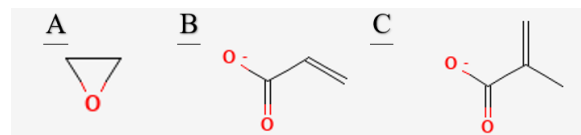


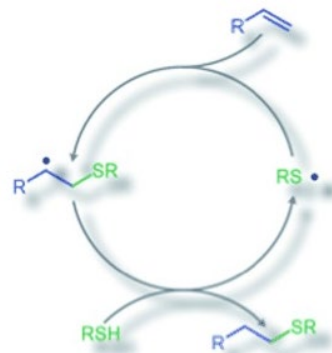
Figure 1. A) Basic epoxide structure<sup>13</sup>, B) acrylate structure<sup>14</sup>, C) methacrylate structure<sup>15</sup>. Structures adapted from Pubchem<sup>13-15</sup>.

VPP resins need to cure quickly to minimize build times, exhibit minimal shrinkage to avoid warped parts, and have a high percentage of precursors converted to polymer at the gel point. Acrylates alone cure very fast, but shrink 5-20%, causing stress and curling. They are typically mixed with methacrylates, which cure more slowly<sup>2</sup>. Epoxide resins for VPP first appeared in patents in 1988. Epoxides are polymerized by a cation-initiated ring opening reaction. This polymerization doesn't cause the number of chemical bonds to change significantly, resulting in only 1-2% shrinkage. Epoxide resins are not inhibited by oxygen, reducing the amount of photoinitiator needed. Despite these benefits, epoxides are rarely used alone because they cure too slowly. Instead, they are often mixed with cationically polymerized vinyl ethers, which cure faster. The fast-curing component of the resin provides structural stability during the build, referred to as "green strength," while the slow curing component reduces shrinkage<sup>2,12</sup>.

Many resins have mixtures of cationic and free radical polymerization systems with varying cure rates. Because the two precursors used do not react together, two separate polymer networks are formed, called an

interpenetrating network. An example is a mixture of acrylates and epoxides. Acrylates polymerize radically, and epoxides cationically. The acrylates react much faster than the epoxides. Early in polymerization, the liquid epoxide monomers act as a plasticizer to the acrylates. The increase in molecular mobility results in a higher conversion rate of the acrylates<sup>12</sup>. However, if the components are not compatible, they may phase separate during the build process.

Another chemical system used in commercial VPP resins is thiol-ene click chemistry<sup>16</sup>. A click reaction produces a non-carbon based linkage with high selectivity, high efficiency, and no by-products<sup>17</sup>. A schematic of the thiol-ene reaction is shown in scheme 1.



Scheme 1. Thiol-ene reaction scheme. Adapted from Hoyle et al<sup>17</sup>.

Thiol-ene systems exhibit step-growth kinetics, in contrast to radical and cationic polymerization systems which exhibit chain-growth kinetics. When a polymer undergoes step growth, any monomer or oligomer has the necessary reactive end groups to react with any other. This contrasts with chain growth, in which a monomer must be activated, and polymerization only occurs at activated sites. Figure 2 shows these two mechanisms.

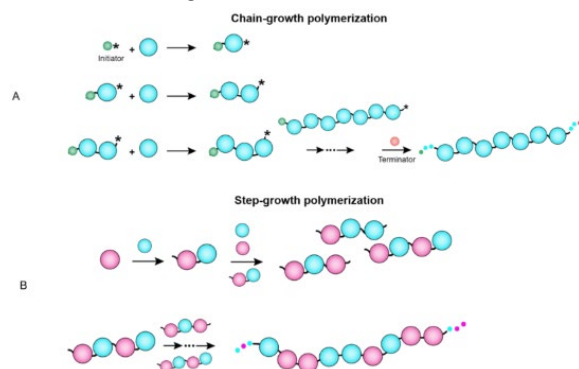


Figure 2. A) Chain growth polymerization, in which propagation is limited to activated chains. B) Step growth polymerization, in which all monomers are free to polymerize with others. Adapted from Esmaili et al<sup>18</sup>.

Step growth polymerization allows a greater conversion rate of monomers to polymers before vitrification, resulting in less shrinkage and shrinkage stresses. In

contrast, acrylate and methacrylate systems undergo chain-growth polymerization. A solely (meth)acrylate resin may reach the gel point at just 20% conversion<sup>2</sup>. Step-growth mechanisms also produce a more homogenous network structure<sup>3,17</sup>. Thiol-ene chemistry also has its disadvantages, including poor storage stability and the bad odor inherent to thiols. Additionally, thiol-ene reactions are not inhibited by oxygen. This is an advantage in many printers, but unsuitable to printers using an oxygen permeable window<sup>19</sup>.

### Elastomer Resins

As AM grows from providing only prototypes to end products, the need for resins with a variety of material properties increases. Compared to other AM technologies, elastomeric resins have proved more challenging for VPP. An elastomer is rubbery in its service temperature range and has high extensibility and low modulus when compared with other polymers. When deformed, these polymers can return to their original shape<sup>20</sup>. Precursors to elastomeric polymers typically have higher viscosity than those to rigid polymers, the cause of which is detailed later in this paper. Unlike other AM technologies, such as direct ink write (DIW), VPP requires low viscosity printing materials, so that the uncured resin can flow quickly and evenly over each completed layer. High viscosity resins may also damage features during recoating. Bottom-up printing requires lower viscosity resins than top-down, typically no higher than 5 MPa<sup>3,21</sup>. Consequently, elastomeric commercial VPP resins are scarce.

Developing elastomeric resins for VPP is challenging because elastomeric properties are dependent on the molecular weight between crosslinks ( $M_c$ ), as shown in figure 4.

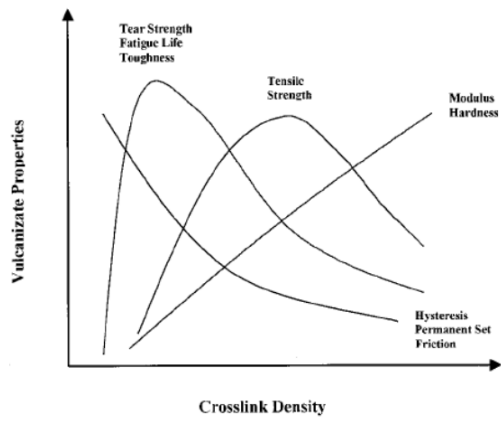


Figure 4. Trends of several polymer mechanical properties of interest plotted against crosslink density. Adapted from Liu et al<sup>26</sup>.

Using tensile modulus as an indicator that a commercial resin produces an elastomer, Sirrine et al estimated that elastomeric resins represent only 7% of resins in the market as of 2016<sup>3</sup>. Elongation at break is another material property that can be useful in evaluating

elastomeric properties. Rigid plastics typically have an elongation at break of <5%, while elastomers typically reach 100% - 1000%. AM resins often fall to the low end of this range, though there are some which are comparable to traditionally manufactured elastomers. Among commercial material options, reported elongations-to-failure include: Carbon3D (380%<sup>22</sup>), a Stratasys resin (up to 230%<sup>23</sup>), and a Formlabs resin (up to 300%<sup>24</sup>). Spectroplast is the outlier, offering silicone resins with up to 1000% elongation at break<sup>25</sup>.

As the average distance between crosslinks increases, the elasticity of the polymer increases. This can be seen in the relationship between molecular weight between crosslinks ( $M_c$ ) and the storage modulus plateau, a measure of the stiffness of the polymer. In a rheological test, a polymer will be subjected to oscillating shear forces with increasing frequency. At low frequencies, the storage and loss modulus curves will be linear. At a certain point, the moduli will plateau and be stable, until the frequency is high enough to damage the molecular structure<sup>26</sup>. A characteristic curve is shown in figure 3 to illustrate these properties.

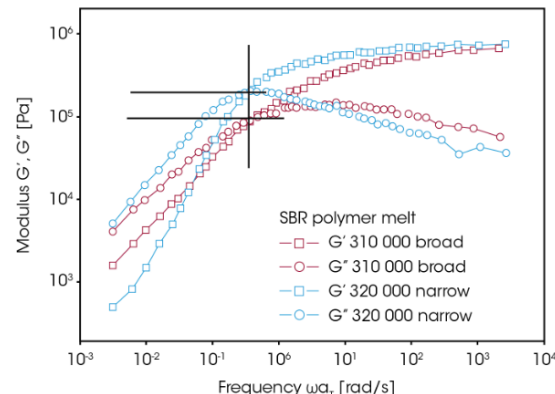


Figure 3. Rheological response of two styrene-butadiene-rubber (SBR) polymer melts, of high ("broad") and low ("narrow") molecular weight distribution.  $G'$  is the storage modulus.  $G''$  is the loss modulus. Adapted from TA Instruments<sup>27</sup>.

An elastomer will have a low storage modulus plateau. The equation relating the plateau shear modulus to  $M_c$  is shown in equation 1.

$$G_N^0 = \frac{\rho RT}{M_c}$$

Equation 1.  $G_N^0$  is the storage modulus plateau,  $\rho$  is the density,  $R$  is the gas constant,  $T$  is the temperature, and  $M_c$  is the molecular weight between crosslinks.

This relationship illustrates a fundamental challenge for formulating low viscosity resins for VPP, because

viscosity is positively correlated with molecular weight. Equation 2 shows that below the molecular weight required for entanglements,  $M_w$  is directly proportional to zero-shear viscosity. Above the molecular weight required for entanglements, this proportionality is given by equation 3<sup>3</sup>. As precursors get larger, viscosity increases, as does the distance between crosslinks. Once the polymer strands are large enough to form entanglements, the viscosity increases even faster.

$$\eta_0 \propto M_w^1$$

Equation 2. Relationship between viscosity and molecular weight, before reaching sufficient molecular weight for entanglement of polymer strands.  $\eta_0$  is the zero-shear viscosity,  $M_w$  is weight average molecular weight.

$$\eta_0 \propto M_w^{3.4}$$

Equation 3. Relationship between viscosity and molecular weight when the polymers are sufficiently large for entanglements to form.

There are a few methods of reducing viscosity without reducing molecular weight. Solvents can reduce viscosity, but they are often toxic and volatile, and they must be removed from the printed objects<sup>3</sup>. To avoid the latter problem, reactive diluents may be used. These are low molecular weight, low viscosity chemicals which are polymerized with the main resin components<sup>28</sup>. Because they participate in the polymerization, they alter the properties of the polymer network. A simpler solution is heating, but this may induce polymerization, especially for acrylates and methacrylates<sup>3</sup>. Other solutions to reducing viscosity include using a mixture of high and low molecular weight precursors, and using novel chemistries with low molecular weight precursors.

#### Functionalized Siloxane Resins

Polysiloxanes are unique among elastomers because of a range of desirable properties. Polydimethylsiloxane (PDMS) has the lowest glass transition temperature of any polymer, is chemically inert, gas permeable, and thermally and oxidatively stable<sup>29</sup>. Although it has a glass transition temperature of -123 °C, PDMS cold crystallizes at approximately -50 °C. This can limit its service temperature range<sup>29</sup>. To make a photopolymerizable silicone resin, PDMS is modified to add functional end groups and/or side chains. These new functional groups enable photopolymerization, in combination with other resin components such as photoinitiators. Silicone based resins are subject to the viscosity problem detailed above, as well as other challenges unique to silicones. For example, the vats

which hold the liquid resin are often made of silicone, and a PDMS based resin can swell into the container. Liners made of polytetrafluoroethylene (PTFE) are commercially available, but builds may still adhere to these liners. Some printer technologies solve this problem, such the oxygen permeable window in CLIP printers. Alternatively, a liquid layer immiscible with the resin or other liners, such as hydrogel film, have been used<sup>32</sup>. The solution depends on the printer and resin.

Commercially available silicone resins include Sil 30 from Carbon3D, which is a silicone urethane. This resin has a reported glass transition temperature of 10 °C, so it is glassy not far below room temperature<sup>30</sup>. Formlabs offers a pure silicone resin, Silicone 40A. This resin has a glass transition temperature of -107 °C<sup>31</sup>. Spectroplast specializes in 3D printing of silicones, but does not sell their resins and provides limited technical specifications<sup>25</sup>. The possibilities for AM silicone based products is highly limited by the scarcity of commercially available resins, as well as the secrecy surrounding their formulations. Research into silicone-based resins is vital for understanding the current AM capabilities as well as future possibilities. The following sections summarize current research into silicone based VPP resins.

#### Methacrylate Functionalization

Elastomeric resins often use the same polymerization strategies as rigid polymer resins. Methacrylates are a common resin component, and as such methacrylated silicones are commercially available. Bhattacharjee et al. used commercial methacrylate functionalized PDMS macromers in a desk-top stereolithography (SL) printer. They used two precursors: PDMS with methacrylate-functionalization only on the end groups (3DP-PDMS-E), and PDMS with methacrylate functionalized side groups (3DP-PDMS-S) to facilitate cross-linking. Varying the ratios of these two precursors (E:S) allow the network and mechanical properties to be tailored. Increasing the E:S ratio increased the strain at break while decreasing the Young's modulus. An E:S ratio of 19:1 had an elongation to break of 159%, and a Young's modulus of 520 kPa. After heating to 120°C for 12 hours, the elongation at break decreased by 33.5%. This is likely due cross-linking initiated by the heat, as is known to happen with thermally cured Sylgard-184, which shows a 29% reduction in elongation to break under the same conditions. Sylgard-184 also shows a 86% increase in Young's modulus, whereas the resin tested showed no statistically significant change<sup>33</sup>. This research demonstrates the range of mechanical properties that can be achieved using off the shelf products. However, the elongation at break achieved is relatively low among elastomers. To improve this, novel chemistries are required.

Du et al. developed a methacrylate functionalized PDMS resin which could attain 1000% elongation before failure. This was done by adding thiourea functional groups to a PDMS with methacrylate end groups. The thiourea groups undergo hydrogen bonding, improving the

elasticity. They used a combination of high molecular weight PDMS at 27k g/mol, and oligomeric PDMS at 0.25k g/mol. The resulting resin had a high viscosity, so two reactive diluents were added, 3-[Tris(trimethylsiloxy)silyl]propyl methacrylate and GENOMER 1122, a monofunctional urethane acrylate. As is often the case, both reactive diluents are toxic<sup>34,35</sup>. This lowered the viscosity from over 100 Pa·s to under 5 Pa·s. Parts printed from this resin had much improved mechanical properties, compared to the methacrylated PDMS. The elongation at break is higher than most commercial resins available for VPP and is comparable to thermally cured silicones. Parts performed well with cyclic strain testing, as well<sup>36</sup>. Novel chemistries can provide improved material properties, but resins may need to be customized to their desired applications.

### Thiol-ene Click Chemistry

As described previously, thiol-ene chemistry is common in VPP printing, and has many desirable properties, such as high efficiency and oxygen insensitivity. The mechanism is shown in scheme 1. Wallin et al. developed a thiol-ene based resin blend containing poly(mercaptopropyl)methylsiloxane-co-dimethylsiloxane (M.S.) and bifunctional vinyl terminated PDMS (V.S.). A low surface energy, high transparency poly-4-methylpentene-1 (PMP) build window was installed to avoid resin swelling into the standard PDMS build window. The crosslink density was controlled by varying the density of the thiol pendant groups on M.S. and the length of the PDMS backbone on the V.S. Researchers achieved a resolution of 50  $\mu\text{m}$  and a build speed of 3 cm/hr. The elastic moduli varied from 6 to 287 kPa. As expected, fewer thiol functional groups on the M.S. and a larger V.S. PDMS backbone produced lower modulus. The objects had an elongation at break of up to 400%, and minimal hysteresis over 100 cycles at 75% strain. Thermal and oxidative stability was not reported, but are known to be problems with thiol-ene chemistry<sup>19</sup>.

PDMS faces its own inherent limitations, such as cold crystallization, whereas bulkier siloxanes do not. Sirrine et al. used a thiol-ene reaction in the vat polymerization of PDMS terpolymers with either diphenylsiloxy (DiPhS) or diethylsiloxy (DiEtS) repeating units, crosslinked with a thiol functionalized PDMS. Structures are shown in Scheme 2.

**Scheme 2.** Left side, above shows a copolymer of DiPhS and PDMS. Left side, below shows a copolymer of DiEtS and PDMS. These copolymers are polymerized with thiol functionalized PDMS, forming a crosslinked terpolymer system. Adapted from Sirrine et al<sup>29</sup>.

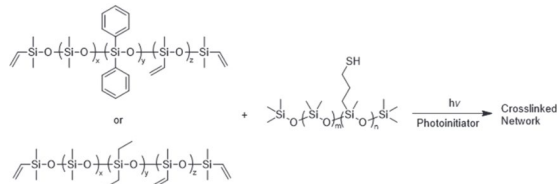
The DiEtS and DiPhS functional groups served to prevent cold crystallization, which PDMS undergoes at -40 to -50  $^{\circ}\text{C}$ <sup>37</sup>. This crystallization limits the functional service range for elastomeric applications. Dynamic mechanical analysis (DMA) showed a small crystallization peak for the DiEtS terpolymer at -70  $^{\circ}\text{C}$ , but this polymer showed an unchanged modulus up to 150  $^{\circ}\text{C}$ . The DiPhS polymer had a stable modulus from -90 to 80  $^{\circ}\text{C}$ <sup>29</sup>, and no crystallization. The resulting photocured polymers had a plateau modulus of approximately 100 kPa. Thermogravimetric analysis (TGA) results show stability in air up to 350 and 360  $^{\circ}\text{C}$  for the DiPhS and DiEtS polymers respectively. In nitrogen, they were stable up to 408 and 390  $^{\circ}\text{C}$  respectively. The printed objects had a feature size of 825  $\mu\text{m}$ , worse than usual for VPP. This can be attributed to the viscosity of the resins. The terpolymer resins had a viscosity approximately twice that of the best performing polymer resin reported by Wallin et al (~0.2 Pa·s vs. 0.089 Pa·s).

### Acrylamide Functionalization

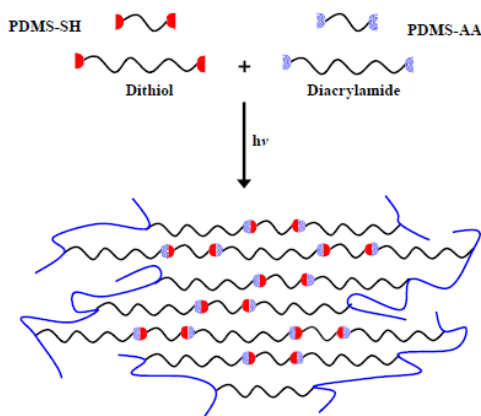
In another example of novel chemistry, Thrasher et al made an acrylamide functionalized PDMS, Bis(propylacrylamide)poly(dimethylsiloxane) (PDMSDMAA). Acrylamides are similar in structure to acrylates, but the ester group is replaced with an amide group. As can be a problem with silicones, the resin swelled into the vat liner. To solve this problem, they used biphasic printing. In this technique, a layer of brine, immiscible with the PDMSDMAA, coats the bottom of the vat. The build stage is positioned above the liquid-liquid interface.

Researchers compared the material properties of parts produced with the PDMSAA resins to three commercial acrylate based elastomeric resins. The resin had a viscosity of 0.291 Pa·s. The cured storage modulus was 174 kPa, comparable to the commercial resins it was compared to. However, the stress strain curve resembles a rigid polymer rather than elastomer. The elongation at break is poor, at just 51%. On the other hand, the glass transition temperature of the PDMSMAA is below -90  $^{\circ}\text{C}$ . A differential scanning calorimetry (DSC) trace shows no endo- or exotherms between -90  $^{\circ}\text{C}$  to 200  $^{\circ}\text{C}$ , indicating that there is no cold crystallization. Taken together, this shows that the PDMSMAA has a good functional service temperature range. Additionally, PDMSDMAA showed minimal anisotropy. Compared to the commercial resins, it had the least difference in tensile stress at 10% strain in perpendicular axes, though the other resins were tested at a much higher strain, 150%<sup>38</sup>.

### Thiol-ene/Acrylamide Combination



As described previously, using two separate polymerization systems can be synergistic. Sirrine et al. describe using resin with thiol-ene and acrylamide functionalized PDMS (PDMA-SH and PDMA-AA respectively). The thiol-ene coupling proceeds linearly, creating long chains. The acrylamide polymerization provides crosslinking. The polymer network formed is depicted in scheme 3.



**Scheme 3.** The precursors are shown above. These are thiol end-group functionalized PDMS and acrylamide end-group functionalized PDMS. Below shows how the thiol and acrylamide groups have linked to produce cross-links in the final polymer network. Adapted from Sirrine et al<sup>3</sup>.

By varying the chain length of both components and the ratio of dithiol to diacrylamide, the storage modulus plateau was varied by an order of magnitude while maintaining a gel fraction over 90%. The 0.75:1.0 M PDMS1.2k-SH:PDMS5.3k-AA mixture had a plateau storage modulus below 0.5 MPa, and an uncured complex viscosity of 0.32 Pa·s, below that of PDMS5.3k-AA alone. The shorter chain-ed PDMS-SH diffused more easily than the longer PDMS-AA, ensuring the thiol-ene chain extension reaction happened faster than the acrylamide polymerization. The viscosity of this resin is higher than other PDMS systems examined in this paper, and so may result in build defects and lower resolution. The objects printed had feature sizes as fine as 150  $\mu$ m. The calculated molecular weight between crosslinks was 12,600 g/mol. These properties demonstrate that this combination can have the properties of much high molecular weight precursors while having a viscosity low enough to be applied to VPP.

A significant downside to this system is its oxygen sensitivity. Tests were conducted in a nitrogen environment. Printing tests showed lower gel fractions than the photorheology tests, likely due to incomplete oxygen removal from the nitrogen sparge. Exposing printed parts to UV after removal from the printing vat increased gel fraction from 80% to 90%, comparable to the photorheology tests. Additionally, some printed

objects contained bubble defects, leftover from the nitrogen sparge. Tensile testing was performed on parts cured on the photorheometer and VPP printed parts which did not undergo post-printing curing. The strain at break of the photorheometer polymerized dogbones was 123% +/- 39%. The printed parts had a strain at break of 80% +/- 10%. Researchers hypothesized that this was due to the lower gel fraction. A range (0.25 to 3 MPa) of plateau storage moduli was achieved by varying the molecular weights and molar ratio of thiol acrylamide functionalized PDMS. The elastic moduli of the printed samples and photocured samples were 400 and 510 kPa respectively, higher than the previously explored thiol-ene system from Wallin et al<sup>3</sup>.

### Future Directions

The summarized research suggests that at the current state of the art, no existing silicone resin can provide all the desirable properties of traditionally manufactured silicone. Low resin viscosity requirements for technologies such as DLP and SL limit the development of elastomeric resins. One as yet unexplored option is to change the printing technology, rather than the resin. Tomographic volumetric printing (TVP) eliminates the need for low viscosity resins. TVP irradiates a volume of resin, rather than a single layer. The volume of the final object is illuminated by multiple beams at multiple angles, curing the object in a single step<sup>39</sup>. In contrast to other VPP technologies, tomographic printing requires high viscosity, transparent resins<sup>40</sup>. In one example, TVP was used to polymerize a thiol-ene based silicone resin, creating parts with feature size of 80  $\mu$ m, and elongation at break of 88%<sup>39</sup>. The technology is not widely available commercially, and doesn't solve the existing problems introduced by modifying silicone to be photopolymerizable. Thiols have poor thermal storage stability, and a bad odor, for example<sup>41</sup>. Methacrylate resins have been shown to lose significant mechanical properties within a week of simulated aging<sup>42</sup>. Instead, novel chemistries are required to create customizable properties. As additive manufacturing expands from rapid prototyping to end-user products, the need for better thermal and mechanical properties increases.

### REFERENCES

- (1) Liu, J.; Ye, J.; Silva Izquierdo, D.; Vinel, A.; Shamsaei, N.; Shao, S. A Review of Machine Learning Techniques for Process and Performance Optimization in Laser Beam Powder Bed Fusion Additive Manufacturing. *Journal of Intelligent Manufacturing* **2023**, *34* (8), 3249–3275. <https://doi.org/10.1007/s10845-022-02012-0>.
- (2) Ligon, S. C.; Liska, R.; Stampfl, J.; Gurr, M.; Mülhaupt, R. Polymers for 3D Printing and Customized Additive Manufacturing. *Chemical*

*Reviews* **2017**, *117* (15), 10212–10290. <https://doi.org/10.1021/acs.chemrev.7b00074>.

(3) Surrine, J. M.; Meenakshisundaram, V.; Moon, N. G.; Scott, P. J.; Mondschein, R. J.; Weiseman, T. F.; Williams, C. B.; Long, T. E. Functional Siloxanes with Photo-Activated, Simultaneous Chain Extension and Crosslinking for Lithography-Based 3D Printing. *Polymer* **2018**, *152*, 25–34. <https://doi.org/10.1016/j.polymer.2018.02.056>.

(4) Hull, C. W. Apparatus for Production of Three-Dimensional Objects by Stereolithography. *4575330*, August 8, 1984.

(5) Bechtold, S. 3D Printing, Intellectual Property and Innovation Policy. *IIC* **2016**, *47* (5), 517–536. <https://doi.org/10.1007/s40319-016-0487-4>.

(6) Tumbleston, J. R.; Shirvanyants, D.; Ermoshkin, N.; Janusziewicz, R.; Johnson, A. R.; Kelly, D.; Chen, K.; Pinschmidt, R.; Rolland, J. P.; Ermoshkin, A.; Samulski, E. T.; DeSimone, J. M. Continuous Liquid Interface Production of 3D Objects. *Science* **2015**, *347* (6228), 1349–1352. <https://doi.org/10.1126/science.aaa2397>.

(7) Desimone, J. M.; ERMOSHKIN, A.; ERMOSHKIN, N.; Samulski, E. T. Continuous Liquid Interphase Printing. *WO2014126837A2*, August 21, 2014. <https://patents.google.com/patent/WO2014126837A2/en> (accessed 2024-02-23).

(8) Desimone, J. M.; ERMOSHKIN, A.; ERMOSHKIN, N.; Samulski, E. T. Method and Apparatus for Three-Dimensional Fabrication with Feed through Carrier. *WO2014126834A3*, November 13, 2014. <https://patents.google.com/patent/WO2014126834A3/en> (accessed 2024-02-23).

(9) Zuev, D. M.; Nguyen, A. K.; Putlyaev, V. I.; Narayan, R. J. 3D Printing and Bioprinting Using Multiphoton Lithography. *Bioprinting* **2020**, *20*, e00090. <https://doi.org/10.1016/j.bprint.2020.e00090>.

(10) Göppert-Mayer, M. Über Elementarakte Mit Zwei Quantensprüngen. *Annalen der Physik* **1931**, *401* (3), 273–294. <https://doi.org/10.1002/andp.19314010303>.

(11) Baldacchini, T. Introduction. In *Three-Dimensional Microfabrication Using Two-photon Polymerization*; Baldacchini, T., Ed.; Micro and Nano Technologies; William Andrew Publishing: Oxford, 2016; pp xxiii–xxvi. <https://doi.org/10.1016/B978-0-323-35321-2.00027-3>.

(12) Gibson, I.; Rosen, D.; Stucker, B. *Additive Manufacturing Technologies: 3D Printing, Rapid Prototyping, and Direct Digital Manufacturing*; Springer New York: New York, NY, 2015. <https://doi.org/10.1007/978-1-4939-2113-3>.

(13) PubChem. *Ethylene Oxide*. <https://pubchem.ncbi.nlm.nih.gov/compound/6354> (accessed 2024-02-26).

(14) PubChem. *Acrylate*. <https://pubchem.ncbi.nlm.nih.gov/compound/25188> (accessed 2024-02-26).

(15) PubChem. *Methacrylate*. <https://pubchem.ncbi.nlm.nih.gov/compound/87595> (accessed 2024-02-26).

(16) Jacobine, A. F.; Rakas, M. A.; Glaser, D. M. Stereolithography Method. *US5167882A*, December 1, 1992. <https://patents.google.com/patent/US5167882A/en?oq=5167882> (accessed 2024-02-23).

(17) Hoyle, C. E.; Bowman, C. N. Thiol–Ene Click Chemistry. *Angewandte Chemie International Edition* **2010**, *49* (9), 1540–1573. <https://doi.org/10.1002/anie.200903924>.

(18) Esmaili, M.; Eldeeb, M. A.; Moosavi-Movahedi, A. A. Current Developments in Native Nanometric Discoidal Membrane Bilayer Formed by Amphipathic Polymers. *Nanomaterials* **2021**, *11* (7), 1771. <https://doi.org/10.3390/nano11071771>.

(19) Wallin, T. J.; Pikul, J. H.; Bodkhe, S.; Peele, B. N.; Murray, B. C. M.; Therriault, D.; McEnerney, B. W.; Dillon, R. P.; Giannelis, E. P.; Shepherd, R. F. Click Chemistry Stereolithography for Soft Robots That Self-Heal. *J. Mater. Chem. B* **2017**, *5* (31), 6249–6255. <https://doi.org/10.1039/C7TB01605K>.

(20) *What are elastomers - Kuraray Specialty Chemicals*. <https://www.elastomer.kuraray.com/blog/what-are-elastomers/> (accessed 2024-02-26).

(21) Hinczewski, C.; Corbel, S.; Chartier, T. Ceramic Suspensions Suitable for Stereolithography. *Journal of the European Ceramic Society* **1998**, *18* (6), 583–590. [https://doi.org/10.1016/S0955-2219\(97\)00186-6](https://doi.org/10.1016/S0955-2219(97)00186-6).

(22) *Elastomeric Materials*. Carbon. <https://www.carbon3d.com/materials/elastomeric> (accessed 2024-02-13).

(23) *Origin® One 3D Printer*. <https://www.stratasys.com/en/3d-printers/printer-catalog/p3/origin-one-printer/> (accessed 2024-02-13).

(24) *Flexible 3D Printing Guide: Compare Processes, Materials, and Applications*. Formlabs. <https://formlabs.com/blog/flexible-3d-printing-materials-and-processes/> (accessed 2024-02-13).

(25) *Technology & Services*. Spectroplast | Silicone 3D Printing Service | Silicone. <https://spectroplast.com/technologyandservices/> (accessed 2024-02-13).

(26) Liu, C.; He, J.; van Ruymbeke, E.; Keunings, R.; Bailly, C. Evaluation of Different Methods for the Determination of the Plateau Modulus and the Entanglement Molecular Weight. *Polymer* **2006**,

47, 4461–4479.  
[https://doi.org/10.1016/j.polymer.2006.04.054.](https://doi.org/10.1016/j.polymer.2006.04.054)

(27) *Introduction to Polymer Melt Rheology and Its Application in Polymer Processing - TA Instruments.*  
<https://www.tainstruments.com/applications-notes/introduction-to-polymer-melt-rheology-and-its-application-in-polymer-processing/> (accessed 2024-03-04).

(28) Malburet, S.; Bertrand, H.; Richard, C.; Lacabanne, C.; Dantras, E.; Graillot, A. Biobased Epoxy Reactive Diluents Prepared from Monophenol Derivatives: Effect on Viscosity and Glass Transition Temperature of Epoxy Resins. *RSC Adv* 13 (22), 15099–15106.  
<https://doi.org/10.1039/d3ra01039b>.

(29) Sirrine, J. M.; Zlatanic, A.; Meenakshisundaram, V.; Messman, J. M.; Williams, C. B.; Dvornic, P. R.; Long, T. E. 3D Printing Amorphous Polysiloxane Terpolymers via Vat Photopolymerization. *Macromolecular Chemistry and Physics* 2019, 220 (4), 1800425.  
<https://doi.org/10.1002/macp.201800425>.

(30) *SIL 30 Silicone Urethane for Wristbands, Headphones & More.* Carbon.  
<https://www.carbon3d.com/materials/sil-30> (accessed 2024-02-13).

(31) *Silicone 40A Resin.* Formlabs.  
<https://formlabs.com/store/materials/silicone-40a-resin/> (accessed 2024-02-13).

(32) Yang, F.; Kazi, A.; Marmo, A.; Grunlan, M. A.; Tai, B. L. Characterizing the Separation Behavior of Photocurable PDMS on a Hydrogel Film during Vat Photopolymerization: A Benchmark Study. *Additive Manufacturing* 2022, 58, 103070.  
<https://doi.org/10.1016/j.addma.2022.103070>.

(33) Bhattacharjee, N.; Parra-Cabrera, C.; Kim, Y. T.; Kuo, A. P.; Folch, A. Desktop-Stereolithography 3D-Printing of a Poly(Dimethylsiloxane)-Based Material with Sylgard-184 Properties. *Advanced Materials* 2018, 30 (22), 1800001.  
<https://doi.org/10.1002/adma.201800001>.

(34) *GENOMER\* 1122 by Rahn USA Corp. - Graphic Arts & Inks.*  
<https://www.ulprospector.com/en/na/Inks/Detail/456/8178/GENOMER-1122> (accessed 2024-02-23).

(35) 3-*Tris(trimethylsiloxy)silyl propyl methacrylate MEHQ + HQ stabilizer, 98 17096-07-0.*  
<http://www.sigmaldrich.com/> (accessed 2024-02-23).

(36) Du, K.; Basuki, J.; Glattauer, V.; Mesnard, C.; Nguyen, A. T.; Alexander, D. L. J.; Hughes, T. C. Digital Light Processing 3D Printing of PDMS-Based Soft and Elastic Materials with Tunable Mechanical Properties. *ACS Appl. Polym. Mater.* 2021, 3 (6), 3049–3059.  
<https://doi.org/10.1021/acsapm.1c00260>.

(37) Kirst, K. U.; Kremer, F.; Pakula, T.; Hollingshurst, J. Molecular Dynamics of Cyclic and Linear Poly(Dimethylsiloxanes). *Colloid Polym Sci* 1994, 272 (11), 1420–1429.  
<https://doi.org/10.1007/BF00654172>.

(38) Thrasher, C. J.; Schwartz, J. J.; Boydston, A. J. Modular Elastomer Photoresins for Digital Light Processing Additive Manufacturing. *ACS Appl. Mater. Interfaces* 2017, 9 (45), 39708–39716.  
<https://doi.org/10.1021/acsami.7b13909>.

(39) Loterie, D.; Delrot, P.; Moser, C. High-Resolution Tomographic Volumetric Additive Manufacturing. *Nat Commun* 2020, 11 (1), 852.  
<https://doi.org/10.1038/s41467-020-14630-4>.

(40) Kelly, B. E.; Bhattacharya, I.; Heidari, H.; Shusteff, M.; Spadaccini, C. M.; Taylor, H. K. Volumetric Additive Manufacturing via Tomographic Reconstruction. *Science* 2019, 363 (6431), 1075–1079.  
<https://doi.org/10.1126/science.aau7114>.

(41) Chen, L.; Wu, Q.; Wei, G.; Liu, R.; Li, Z. Highly Stable Thiol–Ene Systems: From Their Structure–Property Relationship to DLP 3D Printing. *J. Mater. Chem. C* 2018, 6 (43), 11561–11568.  
<https://doi.org/10.1039/C8TC03389G>.

(42) Marin, E.; Boschetto, F.; Zanocco, M.; Doan, H. N.; Sunthar, T. P. M.; Kinashi, K.; Iba, D.; Zhu, W.; Pezzotti, G. UV-Curing and Thermal Ageing of Methacrylated Stereo-Lithographic Resin. *Polymer Degradation and Stability* 2021, 185, 109503.  
<https://doi.org/10.1016/j.polymdegradstab.2021.109503>.